31st Congress of the International Council
of the Aeronautical Sciences

Belo Horizonte, Brazil; September 09-14, 2018

EFFECTS OF NUMERICAL MODELING CHOICES FOR HEATED JETS IN CROSS FLOW

Kelvin C. Morais*, Diego F. Abreu*, Ramon Papa*, Luiz Tobaldini Neto* , Luis Carlos C. Santos*,**
*Embraer S. A., Avenida Brigadeiro Faria Lima, 2170, São José dos Campos-SP, Brazil
** Department of Applied Mathematics, Institut of Mathematics and Statistics, University of São Paulo, Rua do Matão, 1010, São Paulo-SP, Brazil

Keywords: *CFD, Turbulence modeling, Hot Jets in Cross Flow*

Abstract

A numerical investigation of heated jets discharging into a subsonic stream is presented for perpendicular and inclined injection. Numerical results are compared with the experimental temperature distributions for blowing ratios between 0.1 and 2.0. The effects of turbulence models are discussed and improvements on jet spreading and near wall temperature has been noticed for non-linear k-ω models. The alignment of the discharging flow seems to be directly associated with the difficult in predicting the temperature field downstream for every turbulence model. A study on the influence of turbulent Prandtl number and initial turbulent intensity on the spreading rate has also been carried, revealing a weak dependence on both turbulent parameters.

1 Introduction

Jets arranged in crossflow with respect to a main flow are very commonly used in a large number of applications [1]. In the aviation industry two very representative examples are the cooling of turbomachinery blades [2] and auxiliary air outlets of aircraft systems [3, 4]. The goal of blade cooling is to create a film of fluid that keeps the turbine blades below their maximum operational temperatures, whereas auxiliary air outlets are part of subsystems that must provide the required air flow rate for the proper operation of a main system. Some studies available in the literature for auxiliary air outlets are focused in evaluating the total pressure loss (or discharge coefficient) which affects the performance of the air outlet [5, 6]. With that respect, there is a reasonable amount of information for different geometries and operating conditions.

One important parameter used to describe jets in crossflow is the blowing ratio $M = \rho_j U_j / \rho_\infty U_\infty$, which compares the momentum of the jet with the freestream momentum. The Reynolds number is also a relevant parameter in this analysis and the experimental data available in open literature may not cover all range of blowing ratios and Reynolds number of interest. Therefore, having a well validated CFD (Computational Fluid Dynamics) process is not only an important design tool, but also may help fill gaps of information in the literature.

In the mid 70's, Ramsey and Goldstein [8] performed an experimental investigation of the interaction of a heated jet with a deflecting stream at ambient temperature for several jet blowing ratios. Measurements of temperature profiles in several locations downstream the jet exit hole are presented to characterize the three dimensional temperature field with a jet Reynolds number is of the order of 10^4. Another relevant experimental work was conducted by Baldauf et al. [2]. This work has a similar Reynolds number range compared to Ramsey and Goldstein [8] (6800 to 14000), and considers three outlet angles: 30deg, 60deg and 90deg, different temperatures ratios and a range of blowing ratios. The authors present results for local adiabatic effectiveness at the wall. Carlomagno et al. [10] performed a test similar to that conducted by Ramsey and Goldstein [8] with an outlet of smaller diameter and laminar boundary layer. Information about turbulent properties (turbulent kinetic energy and shear stresses) and heat transfer were also reported. The work of Baldauf et al. [2] has been simulated by Harrison and Bogard [12] with different turbulence closure strategies for the Reynolds Averaged Navier-Stokes (RANS) equations. This work has an interesting revision of the literature about simulation of film cooling performance and there is no general recommendation about a unique turbulence model that performs well for all aspects of this problem. In that work, three turbulence models were evaluated, but none of them could provide a good match with experiments for all evaluated parameters. Ivanova et al. [9] evaluated the influence of re-calibrating the values for turbulent Schmidt and Prandtl numbers for jets in crossflow. The RANS results have also been compared with LES (Large-Eddy Simulation) results, which showed a better agreement with experimental data. Goldberg et al. [11] presented an algebraic formulation to account for the turbulent Schmidt and Prandtl number as a field variable. In that work, the method was applied for several flow cases, including a scramjet and impinging jet. Improvements in the simulations were obtained with the proposed formulation.

In the present work some experimental tests are reproduced numerically aiming to assess the ability of turbulence models based on eddy viscosity in simulating jets in crossflow. The ability to use eddy-viscosity based models in RANS simulations is very important in a product development environment, due to its relatively low cost when compared to the very expensive computational resources required to perform analysis using higher fidelity simulations, for example, Large Eddy Simulations (LES).

2 Experimental Data

Numerical results are going to be compared with the experimental data of Ramsey and Goldstein [8]. This experimental study presents results for temperature distribution in the wall and near field for blowing ratios in the range of 0.1 to 2.0 with Reynolds number for the jet of 9.10^3 to 8.10^4. A turbulent boundary layer was reached with a trip wire positioned before the test section. This work was performed for two geometries, one with the air outlet perpendicular to the freestream flow and other with the outlet inclined 35deg with respect to the freestream flow.

3 Numerical Methods

The commercial software CFD++ [13], from Metacomp Technologies, has been used in the present work. Steady state simulations were performed using a preconditioned density-based solver for the RANS equations. A second-order spatial discretization scheme and an implicit time integration has been used. Linear and non-linear turbulence models were tested. The realizable k-ε [16] and SST [14] were the selected linear models, while the cubic k-ε [17] and Hellsten [15] were the selected non-linear turbulence models. The use of shell conduction was also briefly assessed using the software Fluent with a pressure-based solver in a coupled, pseudo-transient formulation.

3.1 Computational Domain

The computational domain comprises a cylindrical duct discharging the heated jet into a flat plate freestream. Two configurations are analyzed in terms of discharging angle: 90deg and 35deg. Geometrical dimensions follow the experimental assembly of Ramsey and Goldstein [8], presented in Figure 1. The flat plate length was determined to reproduce the same boundary layer displacement thickness of the experiment in the duct exit station. The duct length was designed to achieve a fully developed flow before the exit.

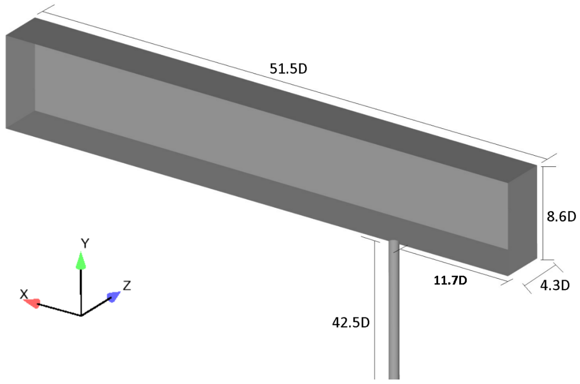

Fig. 1 Numerical domain

3.2 Computational Mesh and Boundary Conditions

A mesh dependence study has been carried out in order to define the computational grid used in this work. In this study, grid topology and refinement were investigated and the meshes were evaluated primarily according to their accuracy in capturing the main flow features. An unstructured hybrid mesh of 50M cells was selected for the present study. This mesh is composed of prismatic elements near the walls to capture the boundary layer behavior and tetrahedral elements filling the volume domain not covered by prismatic cells. At the walls, the first normal cell distance was limited to ensure $y^+ < 1$ for every wall surface. At the heated jet outlet, a refinement region was created surrounding the jet mixture zone. The boundary conditions were selected aiming to reproduce the wind tunnel experiment of Ramsey and Goldstein [8]. For the external flow, a normal temperature-velocity boundary condition was used on the external flow inlet and a simple back pressure condition was imposed at the domain outlet. To reproduce the internal flow in the duct and keep a specific blowing ratio between internal and external flows, the temperature velocity boundary condition has also been used for the internal flow inlet. The wind tunnel walls were all modeled as adiabatic wall. The problem is considered symmetric on the spanwise direction. Thus, a symmetry plane was included so that only half of the experimental geometry is meshed.

4 Results and Discussions

Results are going to be divided in 3 sections. The first section concerns the improvements achieved with different turbulence models. Second section presents a study on the sensitiveness of turbulent Prandtl number and the use of variable Prandtl number with *cubic* $k-\varepsilon$ turbulence model. A brief comment is made on the effects of turbulent intensity at the inlets and the effect of shell conduction at the lower wall.

In this work, temperature is considered by means of a non-dimensional parameter, defined as follows:

$$\eta_T = \frac{T - T_\infty}{T_{Jet} - T_\infty}.$$

A set of parameters of interest are defined to help the assessment of the quality of the numerical results. These parameters are depicted in Figure 2 and represent the main features of the shape of the temperature profiles. The main parameters of interest are the wall temperature, the peak temperature and the y-location of the peak temperature. Also of some importance is the y-location where T_1 is reached (jet boundary).

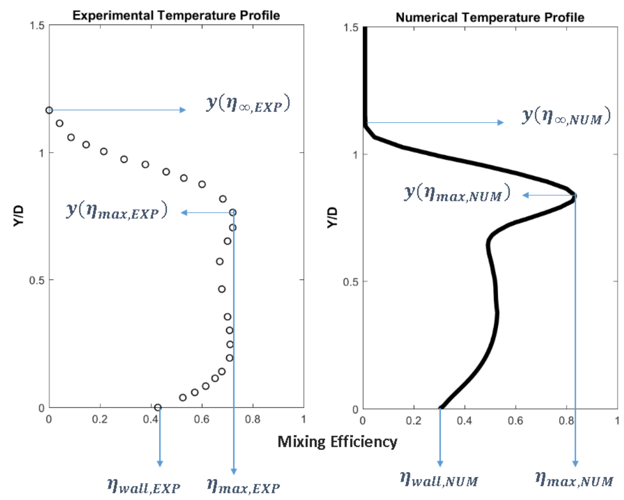

Fig. 2 Graphical example of the set of parameters of interest

4.1 Turbulence Models

The numerical simulations were compared to the experimental data for two different geometries, outlet duct with angles of 90deg and 35deg to mainstream flow. The perpendicular outlet was tested with four blowing ratios: 0.1, 0.5, 1.0 and 2.0, while the 35deg outlet has been tested for blowing ratios 1.0 and 2.0. Figures 3, 4, 5 and 6 present the results for the perpendicular outlet and Figures 7 and 8 present the results for the 35deg outlet.

Investigating the result for the lowest blowing ratio for the perpendicular outlet, Figure 3, it is observed that the wall temperature is overestimated numerically for all models. The non-dimensional wall temperature obtained in the simulations is consistently higher than the experimental results at all the stations at x/D=0. Moving spanwise to z/D=0.5, larger differences are observed only at the first x/D station. At the other stations, the numerical results present similar or smaller temperatures. The different turbulence models provided very similar results.

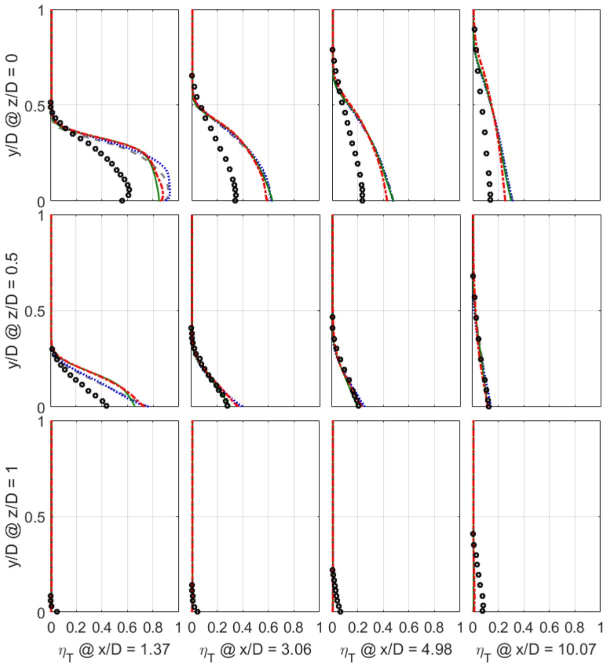

Fig. 3 Non-dimensional temperature distribution for the 90deg outlet with a blowing ratio of 0.1. Realizable k-ε (- -), SST (· · ·), cubic k-ε (—), Hellsten (- · · -) and experimental data (**o**)

The results for blowing ratio 0.5, Figure 4, show a better agreement between the numerical and experimental results for the temperature at the wall when compared to the blowing ratio 0.1. The differences between the selected different models are now more pronounced than they were for the blowing ratio 0.1. The simulated peak temperature is higher than the experimental values up to z/D=0.5, however for z/D=1 the numerical temperature values tend to be lower than the experiment. These observations lead to a conclusion that the numerical results are tending to promote a slower mixing of the secondary jet flow with the external flow, with a higher persisting peak at the jet center plane and a slower decay spanwise.

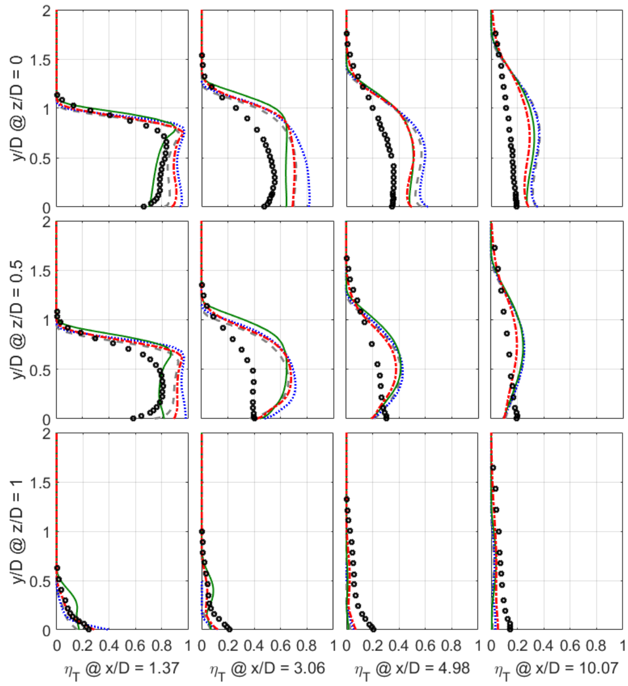

Fig. 4 Non-dimensional temperature distribution for the 90deg outlet with a blowing ratio of 0.5. Realizable k-ε (- -), SST (· · ·), cubic k-ε (—), Hellsten (- · · -) and experimental data (**o**)

Increasing the blowing ratio to 1.0 for the perpendicular outlet, seen in Figure 5, an even better agreement for the temperature at the jet center plane, z/D=0 is obtained. SST and Hellsten turbulence models could provide exactly the same wall temperature of the experiment. The temperature distributions for the stations at z/D = 0.5 still present higher values of temperature, but the differences are smaller than those seen for the blowing ratio 0.5. The temperature spreading has increased, because of the higher blowing ratio but the lack of experimental data at stations with $z/D > 1.0$ do not allow a comparison of the models behavior at the jet boundaries. For this blowing ratio, at stations $z/D = 1.0$, it is possible to observe high temperatures and a behavior similar to what was observed for blowing ratio 0.5 at stations $z/D = 0.5$, large differences close to the mid of the jet. The numerical results with all the tested models are providing temperature profiles with limited agreement with the experiment. The largest differences are obtained as on moves away from the outlet in both x- and z-direction. The Hellsten model seems to promote the largest level of mixing between all evaluated models.

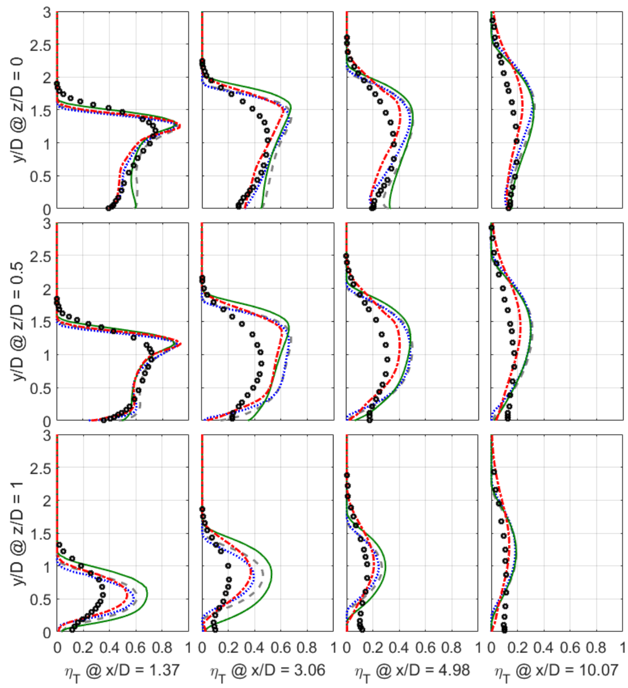

Fig. 5 Non-dimensional temperature distribution for the 90deg outlet with a blowing ratio of 1.0. Realizable k-ε (- -), SST (· · ·), cubic k-ε (—), Hellsten (- · · -) and experimental data (**o**)

For the highest blowing ratio with the perpendicular outlet, Figure 6, the temperature at the wall is well captured. In this case, the matching of the wall temperature is mainly due to the lack of heating seen at the wall due to the large vertical lifting of the jet. The simulation results show a two-peaked temperature profile, whereas the experimental results indicate a more subtle secondary peak, with an almost monotonic variation up to the peak temperature value in y/D. For this blowing ratio the difference between the turbulence models are larger than the obtained for blowing ratio 1.0. The predicted y-location of the peak temperature is different among the tested models. Once more it is possible to observe a higher level of temperature spreading for the Hellsten model, leading to a better agreement with the experimental results.

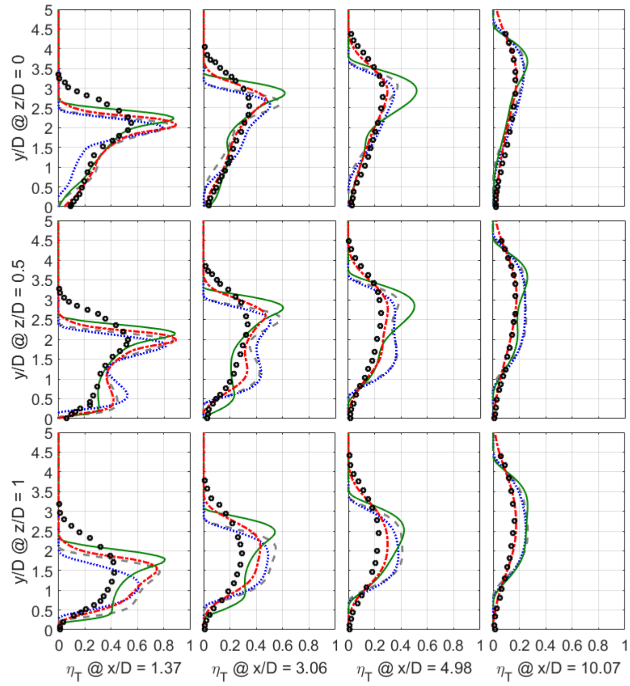

Fig. 6 Non-dimensional temperature distribution for the 90deg outlet with a blowing ratio of 2.0. Realizable k-ε (- -), SST (· · ·), cubic k-ε (—), Hellsten (- · · -) and experimental data (**o**)

Investigating the results for the 35deg outlet for both 1.0 and 2.0 blowing ratios, Figures 7 and 8, it is possible to observe a better agreement between simulation and experimental results. The peak temperature is, however, still overestimated, for all turbulence models. The y-location of the peak temperature is also higher than those obtained in the experiment. The results for the blowing ratio 2.0 also presents more differences in the temperature profile among the turbulence models, as seen for the 90deg outlet. Also, as seen for the perpendicular outlet results, a two-peaked temperature profile is observed. The position of both temperature peaks and their values are different than the experimental results.

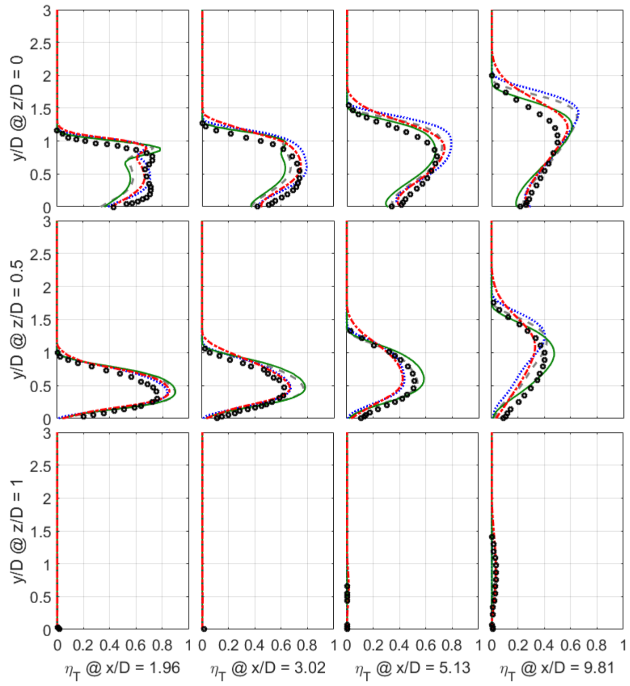

Fig. 7 Non-dimensional temperature distribution for the 35deg outlet with a blowing ratio of 1.0. Realizable k-ε (- -), SST (· · ·), cubic k-ε (—), Hellsten (- · · -) and experimental data (**o**)

In general, it is possible to observe that the jet trajectory, which is characterized by the y-location of the peak temperature at the center plane, tends to be higher in the numerical results than in the experiments. Moving farther from duct outlet, the differences between simulations and experiments increase.

Concerning the wall temperature, it is observed that for small values of blowing ratios the value of the temperature is over-predicted by the numerical models. Increasing the blowing ratio, the difference between the simulations and experimental results decreases. For high blowing ratios no difference is observed due to the small influence of secondary flow temperature in the wall.

The use of non-linear turbulence models introduced some new features in the numerical

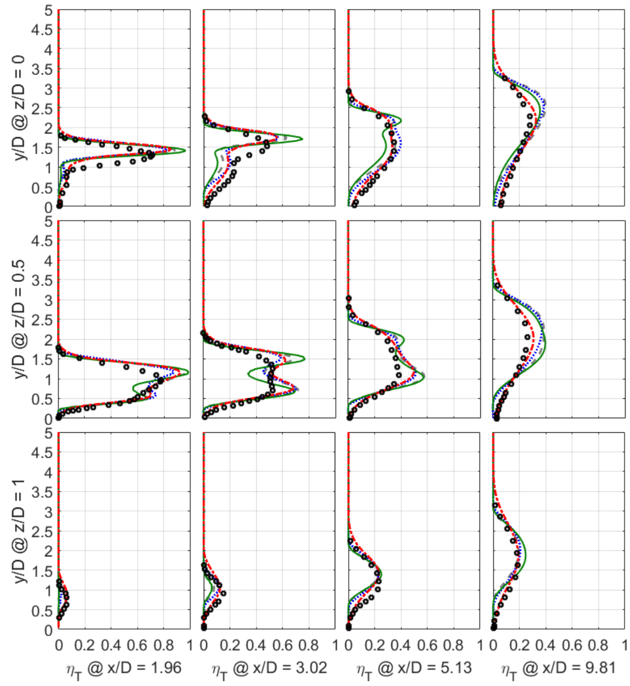

Fig. 8 Non-dimensional temperature distribution for the 35deg outlet with a blowing ratio of 2.0. Realizable k-ε (- -), SST (· · ·), cubic k-ε (—), Hellsten (- · · -) and experimental data (**o**)

temperature profile shapes which were not obtainable with the linear models. Comparing the results for the realizable k-ε with the cubic k-ε, it is seen that cubic k-ε consistently provides a smaller temperature in the centerline, while the temperature is higher at other z/D stations, these phenomena are associated with an enhanced spreading of temperature.

The Hellsten model presented a better agreement with the experimental results. Close to the duct outlet, the temperature values of Hellsten model are similar to what is obtained from the other models. Moving downstream the jet outlet, the results from Hellsten model present temperature values that are similar or below those of the experiment. Comparing the results of turbulent to laminar viscosity ratio, Figure 9, it is possible to see that the amount of turbulent eddy viscosity generated with the Hellsten model is higher than what is produced with the other models. This result is direct related to the increased spreading rate observed in the temperature profiles with this model.

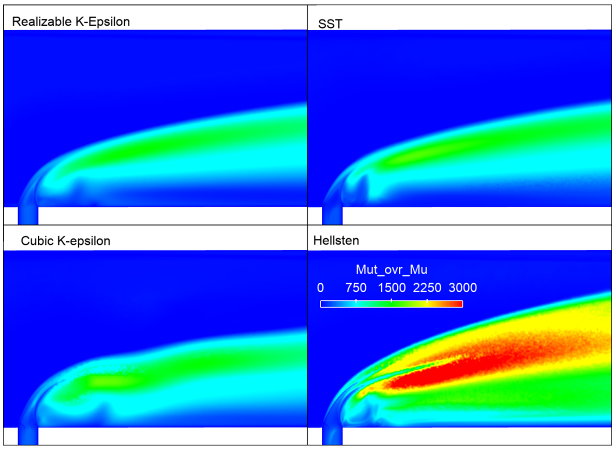

Fig. 9 Comparison of μ_t/μ for different turbulence models in the symmetry plane

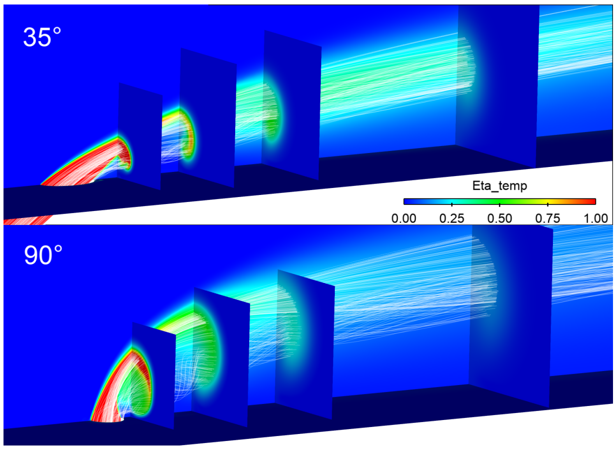

Fig. 10 Comparative view of the flow for the two geometries for a blowing ratio of 2.0

This high spreading rate observed can be related to the results provided by Hellsten [15]. In that work the author performs the comparison of the Hellsten models with other k-ω models and with experiment for the spreading rate of wake, mixing layer, plane and round jets. It was observed an adequate spreading rate, similar to the experimental data, for the wake and the mixing layer, and an excessive spreading rate for the plane and round jets. The author discuss that this excessive spreading rates for jet flows was related to lack of specific calibration for these problems, which could lead to compromised results for other problems. The results from other turbulence models show a reduced spreading rate when compared to experimental data. The increased level of turbulent eddy viscosity provided by the Hellsten models seems to increase the jet spreading rate obtained the problem of jets in crossflow, and, in this case, leading to a better agreement with experimental data.

Comparing the results from the two duct geometries, with angles of 90deg and 35deg, it is observed a better agreement to the experimental data for the 35deg outlet. The comparatively larger alignment between the outlet and the main flow promotes less interference of the jet in the external flow compared do the 90deg outlet. Figure 10 shows a comparison between the flows of the two geometries for a blowing ratio of 2.0.

4.2 Turbulent Prandtl number

The effect of the turbulent Prandtl number is presented in figure 11. For this study, baselines simulations were done with Pr_T=0.8 and variations under the range 0.7 to 1.16 were also performed in order to verify the sensitivity of numerical results to that parameter. Simulations were performed for realizable k-ε and Hellsten turbulence models, for both 90deg and 35deg duct. Blowing ratios from 0.5 to 2.0 were simulated for the perpendicular outlet and 1.0 and 2.0 for the inclined outlet. It was observed that the turbulent Prandtl number effect was similar for all test cases.

Numerical results with larger turbulent Prandtl number presents higher temperature peaks near the symmetry plane, at stations z/D=0 and z/D=0.5. As one moves away from this plane, at station z/D=1.0 for example, the trend is inverse. That is, simulations with larger values of turbulent Prandtl number are showing lower levels of temperature far from the jet center plane. In terms of the y-location of the temperature peak, minor effects are observed between the simulations. The same is observed for the wall temperature, which is almost the same for the three cases analyzed. The trends seen in these simulations are a direct effect of reduction in the temperature diffusion rate with the increase in the turbulent Prandtl number.

For cubic k-ε turbulence model, a dynami-

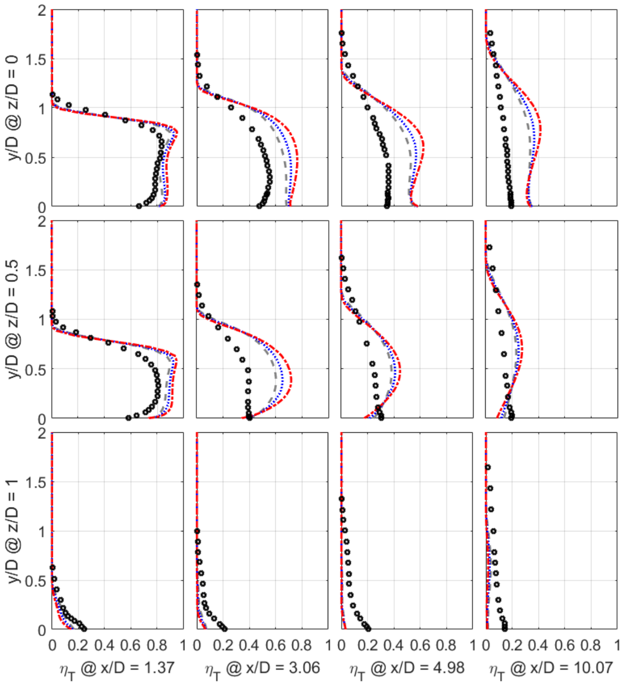

Fig. 11 Non-dimensional temperature distribution for the 90deg outlet with a blowing ratio of 0.5. Turbulent Prandtl number 0.7 (- -), Turbulent Prandtl number 0.88 (···), Turbulent Prandtl number 1.16 (- · -) and experimental data (**o**)

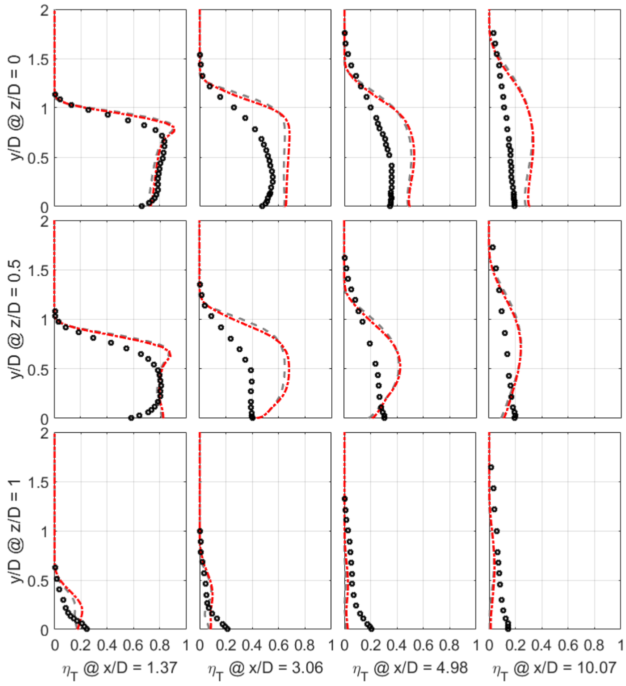

Fig. 12 Non-dimensional temperature distribution for the 90deg outlet with a blowing ratio of 0.5. Cubic k-ε with fixed Prandtl number of 0.88 (- -), Cubic k-ε with variable Turbulent Prandtl number (- · -) and experimental data (**o**)

cally varying turbulent Prandtl number is also available in the CFD solver. An algebraic Reynolds stress model is used to include the turbulent Prandtl number as a field variable [11]. This model was also simulated for normal and inclined injection for several blowing ratios and its influence in numerical results was found to be small for all test cases. Numerical results with variable and fixed turbulent Prandtl number are compared in figure 12.

The temperature profiles from simulations with variable and fixed turbulent Prandtl number show minor differences among them. The differences are due to the increase in the turbulent Prandtl number in the variable model, producing jets with different spreading rates. The variable turbulent Prandtl number model did not improve the predictions for this particular study.

The effect of varying the turbulent Prandtl number for this problem was found to be of secondary importance in influencing the temperature distribution. Furthermore, considering that turbulent Prandtl number lies near 0.9 for general flows [11], there is little justification to impose different global values for this case. The analysis presented here should be regarded mostly as a sensitivity assessment only.

4.3 Other effects studied

A sensitivity study has been carried out increasing the ratio of turbulent to laminar viscosity in the flat plate inlet. The tests used a baseline value and a value 4 times higher than that used as baseline. Almost no effect has been noticed for this test in terms of temperature downstream the jet mixture zone. Numerical results indicate that in the mixture zone the ratio of turbulent to laminar viscosity is more than 10 times the inlet value and the turbulence produced by the jets interaction seems to dominate the mixture process downstream. Also, in order to evaluate the need for modeling the heat conduction in the walls, an investigation for blowing ratio 0.5 was performed using shell conduction. As the experimental work do not provide information about wind tunnel walls in terms of thickness and conductivity, some values were freely assumed to perform the study. The effects of wall conduction in the temperature profiles were restricted to the near wall region. Minor differences in the temperature field have been noticed close to the jet center line. As expected, a more uniform temperature distribution was observed in the walls due to heat conduction on the walls.

5 Conclusions

In the present study the effect of numerical modeling choices for the problem of a hot jet in crossflow was verified. Four different turbulence models were analyzed in a range of blowing ratios from 0.1 to 2.0. Two different injection angles were also evaluated. The influence of the turbulent Prandtl number, turbulent intensity level and shell conduction were additionally considered.

For all turbulence models the numerical results indicate an insufficient level of mixing between the two jets, with limited spanwise temperature decay and, in many cases, showing higher temperature peaks. The use of non-linear turbulence models, in particular the Hellsten $k-\omega$ variation, tended to improve the numerical predictions. For lower values of blowing ratio the wall temperature is over-predicted, whereas increasing the blowing ratio usually leads to a better agreement between the numerical results and experimental values. In general, it can be argued that many engineering applications may find that the level of agreement achieved between numerical and experimental results is sufficient.

References

[1] Zhang, L., Yang, V., Flow Dynamics and Mixing of a Transverse Jet in Crossflow - Part 1: Steady Crossflow, *Journal of Engineering for Gas Turbines and Power*, Vol. 139, 2017.

[2] Baldauf, S., Schulz, A., Wittig, S., High-Resolution Measurements of Local Effectiveness From Discrete Hole Film Cooling, *Journal of Turbomachinery*, Vol. 123, pp. 758-765, 2001.

[3] Jesus, A. B., Takase, V. L., Vinagre, H. T. M., CFD Evaluation of the Discharge Coefficient of Air Outlets in the Presence of an External Flow, *Proceedings of the 10th Brazilian Congress of Thermal Sciences and Engineering*, 2004.

[4] Benard, E., Watterson, J. K., Gault, R., Richardson, J., Review and Experimental Survey Of Flapped Exhaust Performance, *Journal of Aircraft*, Vol. 45, No. 1, pp. 349-352, 2008.

[5] Dewey, P. E., *A Preliminary Investigation on Aerodynamic Characteristics of Small Inclined Air Outlets at Transonic Mach Numbers*, NACA Technical Note 3442, 1955.

[6] Dewey, P. E., Vick, A. R., *An Investigation of the Discharge and Drag Characteristics of Auxiliary-Air Discharging into a Transonic Stream*, NACA Technical Note 3466, 1955.

[7] Lighter and stronger materials for greener aircraft, *https://ec.europa.eu/programmes/horizon2020/en/news/lighter-and-stronger-materials-greener-aircraft*, Accessed: 2017-07-13.

[8] Ramsey, J. W., Goldstein, R. J., *Interaction of a Heated Jet with a Deflecting Stream*, NASA CR-72613, 1970.

[9] Ivanova, E. Noll, B., Aigner, M., A Numerical Study on the Turbulent Schmidt Numbers in a Jet in Crossflow, *Proceedings of ASME Turbo Expo*, 2012.

[10] Carlomagno, G. M., Nese, F. G., Astarita, T., PIV and Wall Convective Heat Transfer Measurements in a Round Jet in Cross-Flow, 24th International Confress of The Aeronautical Sciences, ICAS, 2004

[11] Goldberg, U.C., Palaniswamy, S., Batten, P., Gupta, V., Variable Turbulent Schmidt and Prandtl Number Modeling, *Engineering Applications of Computational Fluid Mechanics*, Vol. 4, No. 4, pp 511-520, 2010.

[12] Harrison, K. L., Bogard, D. G., Comparison of RANS Turbulence Models for Prediction of Film Cooling Performance, *Proceedings of ASME Turbo Expo*, 2008.

[13] Chakravarthy, S., A unified-grid finite volume formulation for Computational Fluid Dynamics, *International Journal for Numerical Methods in Fluids*, Vol.31, pp 309-323, 1999.

[14] Menter, F.R., Two-Equation Eddy-Viscosity Turbulence Models for Engineering Applications, *AIAA Journal*, Vol. 32, No. 8, 1994.

[15] Hellsten, A., New Advanced k-ω Turbulence Model for High-Lift Aerodynamics *AIAA Journal*, Vol. 43, No. 9, 2005.

[16] Shih, T.H., Liou, W.W., Shabbir, A., Yang, Z., Zhu, J., *A new k-ε Eddy Viscosity Model for High Reynolds Number Turbulent Flows - Model Development and Validation*, NASA Technical Memorandum 106721, 1994.

[17] Craft, T.J., Launder, B.E., Suga, K., Development and Application of a Cubic Eddy-Viscosity Model of turbulence, *International Journal of Heat and Fluid Flow*, Vol. 17, pp 108-115, 1996.

Contact Author Email Address

kelvin.morais@embraer.com.br

Copyright Statement